

## Geodesics, complexity and holography in (A)dS<sub>2</sub>

---

**Damián A. Galante**<sup>a,\*</sup>

<sup>a</sup>*King's College London, the Strand, London WC2R 2LS, UK*

*E-mail:* [damian.galante@kcl.ac.uk](mailto:damian.galante@kcl.ac.uk)

We consider spacelike geodesics in two-dimensional spacetimes. In the case of the AdS<sub>2</sub> black hole, their length increases linearly with time for long times, compared to the inverse temperature. In dS<sub>2</sub>, spacelike geodesics anchored at the same time, only exist at  $t = 0$ . To interpret this result holographically, we embed a patch of dS<sub>2</sub> inside an AdS<sub>2</sub> spacetime. In that case, geodesics only exist for a time of order the inverse temperature and their length decreases with time. We comment on possible implications of this result in terms of two-point correlators and holographic complexity.

*Corfu Summer Institute 2021 "School and Workshops on Elementary Particle Physics and Gravity"  
29 August - 9 October 2021  
Corfu, Greece*

---

\*Speaker

## 1. Introduction

The aim of this short note is to summarise some recent progress in trying to understand the holographic nature of the cosmological event horizon in de Sitter (dS) space, the maximally symmetric solution to Einstein's equations with a positive cosmological constant. See [1, 2] for reviews. The metric of dS space in  $d$  dimensions is given by,

$$ds^2 = -d\tau^2 + \ell^2 \cosh^2\left(\frac{\tau}{\ell}\right) d\Omega_{d-1}^2, \quad (1)$$

where  $\ell$  is the radius of dS and  $\tau$  is the global time coordinate, and  $d\Omega_{d-1}$  is the metric on the  $(d-1)$ -unit sphere. From now onwards, we will set  $\ell = 1$ . Due to the ever-accelerated expansion of the spacetime and the finite speed of light, observers in dS are surrounded by a cosmological event horizon. In fact, the region that is causally accessible to an observer in a dS space is called the static patch and is given by

$$ds^2 = -(1-r^2)dt^2 + \frac{dr^2}{1-r^2} + r^2 d\Omega_{d-2}^2. \quad (2)$$

Note the appearance of a horizon at  $r_h = 1$ . Given that the AdS/CFT correspondence has proven to be a fundamental tool to understand black hole event horizons, we would like to apply the same tools to the case of the cosmological horizon.

However, one of the main problems in doing so is that the static patch region does not have any asymptotically-large region where to anchor observables, as in the AdS case. The radial coordinate  $r$  in eq. (2) goes from  $r = 0$  at the observer's worldline to  $r = 1$  at the horizon, while the usual radial coordinate in AdS goes to  $r \rightarrow \infty$ , as it reaches the AdS boundary.

This problem was recently overcome by the construction of the centaur geometry [3, 4], a two-dimensional geometry that is asymptotically AdS but, in the interior, it interpolates to part of a dS static patch with a cosmological horizon. This construction opens the possibility of using the usual tools used in holography to probe the cosmological horizon, see next section.

One of such probes are spacelike geodesics. These are interesting for a variety of reasons. Even before going into holography, geodesics are useful tools to compute two-point functions in curved spacetimes. Consider a free massive scalar field  $\phi$  with mass  $m$  in a fixed curved background. Following the worldline formalism, one can schematically compute the two-point function for the scalar field by doing the following path integral,

$$\langle \phi(x)\phi(x') \rangle = \int D\mathcal{P} e^{-mL[\mathcal{P}]} \approx \sum_{\text{geodesics}} e^{-mL_g}, \quad (3)$$

where we need to path-integrate over all possible paths  $\mathcal{P}$  connecting the two points and  $L[\mathcal{P}]$  is the length of that path [5]. The last expression is the saddle-point approximation when  $m \rightarrow \infty$  and the length reduces to the geodesic length  $L_g$ . In this limit, essentially, computing the length of geodesics gives (the logarithm of) the two-point function of the scalar field.

In the case where the spacetime is asymptotically AdS, one can further connect this two-point function to the conformal two-point function of boundary operators. This was initially computed in [5, 6] for AdS<sub>3</sub>, finding agreement with CFT expectations.

In the case of  $dS$ , the two-point function is known analytically in every dimension and for any mass of the scalar field. In the Bunch-Davies vacuum, the exact two-point function is given by [1, 2],

$$\langle \phi(x)\phi(x') \rangle_{dS} = \frac{\Gamma(h_+)\Gamma(h_-)}{(4\pi)^{d/2}\Gamma\left(\frac{d}{2}\right)} {}_2F_1\left(h_+, h_-; \frac{d}{2}; \frac{1+P}{2}\right), \quad h_{\pm} = \frac{(d-1)}{2} \pm \sqrt{\left(\frac{d-1}{2}\right)^2 - m^2}, \quad (4)$$

where  $P$  is defined in embedding coordinates as  $P = \eta_{ij}X^iX^j$ , with  $X$  being the coordinates of  $x$  in  $(d+1)$ -Minkowski spacetime. In  $d=2$ , when the two points are located at the south and north pole of the circle at a given time  $t$ , and, in the large-mass limit, this expression reduces to [7]

$$\langle \phi_N(t)\phi_S(t) \rangle_{dS_2} \approx \frac{e^{-m\pi}}{2} \sqrt{\frac{2}{m\pi \sinh 2t}} \sin(2mt + \pi/4). \quad (5)$$

It would be interesting to reproduce this two-point function from a geodesic calculation in  $dS$  space. See comments in the next section.

Geodesics also appear in a variety of contexts in holography. For instance, in  $d=3$ , they are co-dimension two extremal surfaces, and as such, they compute entanglement entropies through the Ryu-Takayanagi formula [8]. In most of this note, we will be interested in the case of  $d=2$ , where geodesics are co-dimension one. These objects are conjectured to compute a holographic complexity via the relation [9, 10],<sup>1</sup>

$$C_V = \max \frac{L_g}{G_N}, \quad (6)$$

where  $G_N$  is the Newton's constant. In the dual quantum theory, this measure gives some notion of how hard is to construct the quantum state, given a reference state and a set of simple operations. See [11] for a recent review.

In the next section, we will show how to compute the length of spacelike geodesics in  $AdS_2$ ,  $dS_2$  and the centaur geometry and interpret the results in view of the aforementioned quantum measures.

## 2. Geodesics

It is a simple exercise to compute geodesics in two-dimensional spacetimes. In particular, we will be interested in spacetimes with a metric given by

$$ds^2 = -f(r)dt^2 + \frac{dr^2}{f(r)} = -f(r)dv^2 + 2dvdr, \quad (7)$$

where in the last equality we introduced the null coordinate  $dv \equiv dt + dr/f(r)$ . Usually these metrics can be extended to two-sided geometries and we will be interested in computing geodesics that are anchored at opposite sides of the Penrose diagram. See fig. 1. The isometries of our geometries imply that the length is invariant under the following change of the boundary times

<sup>1</sup>The  $V$  subscript refers to volume in  $d$ -dimensions but in  $d=2$  this is actually the geodesic length.

$t_R \rightarrow t_R + \Delta t$  and  $t_L \rightarrow t_L - \Delta t$  and hence only depends on the combination  $t_L + t_R$ . For simplicity, we will assume a symmetric configuration of the boundary times,  $t_L = t_R = t/2$ . We refer the reader to [12] for details on the computations. In this section, we will just state the main results.

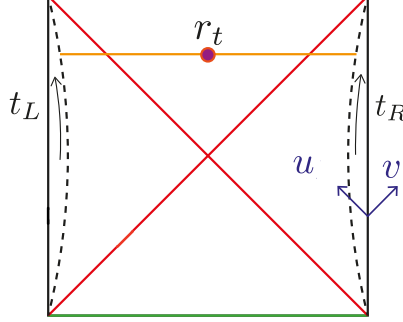


**Figure 1:** Generic Penrose diagram for the geometries under consideration. The boundary  $r = R_b$  is indicated by a dashed black line. The times  $t_L = t_R$  run upwards along both boundaries. We have also illustrated a geodesic with turning point  $r_t$ . Figure adapted from [12].

The geodesics can be studied using the following length functional,

$$L = \int ds \sqrt{-f(r)\dot{v}^2 + 2\dot{v}\dot{r}}, \quad (8)$$

where both coordinates  $r$  and  $v$  are written in terms of a parameter  $s$  and the dot indicates derivative with respect to  $s$ . It is straightforward to verify that the length does not depend explicitly on  $v$ , so we can define a conserved quantity  $P \equiv -f\dot{v} + \dot{r}$ , associated to this symmetry. The length and the time at which the geodesics are anchored can be both written in terms of this parameter  $P$  as,

$$L(P) = 2 \int_{r_t}^{R_b} \frac{dr}{\sqrt{f(r) + P^2}}, \quad t(P)/2 = r_t^* - r^*(R_b) + \int_{r_t}^{R_b} dr \left( \frac{\sqrt{f(r) + P^2} - P}{f(r)\sqrt{f(r) + P^2}} \right), \quad (9)$$

where  $r_t$  is the position of the turning point, given by  $f(r_t) + P^2 = 0$ , see fig. 1.  $R_b$  is a point close to boundary (or worldline in the case of dS) and the tortoise coordinate is defined by  $dr^* = dr/f(r)$ . For a given  $f(r)$ , eq. (9) gives both the length and the time as a function of  $P$ . At least parametrically, this gives the length as a function of the time they are anchored at. Furthermore, if  $t(P)$  can be inverted, then we can get an explicit expression for  $L(t)$ .

## 2.1 Geodesics in (A)dS<sub>2</sub>

We can now specify  $f(r)$  to obtain specific expressions for the different geometries. We start with the case of the AdS<sub>2</sub> black hole, which is given by  $f(r) = r^2 - 1$ . We are fixing here the inverse temperature to  $\beta = 2\pi$ . This problem has been studied in [13]. It is known that geodesics in this spacetime are the geodesics of global AdS<sub>2</sub> anchored at the same time, so they are horizontal lines in the Penrose diagram, see fig. 2(a). Performing the integrals (9) and restoring the dependence on  $\beta$ , we obtain that in this case,

$$L(t)_{\text{BH}} = 2 \operatorname{arccosh} \left( \sqrt{(R_b^2 - 1) \cosh^2 \frac{\pi t}{\beta} + 1} \right) \sim 2 \log \left( 2R_b \cosh \frac{\pi t}{\beta} \right) + O(1/R_b^2). \quad (10)$$

The length, as usual in AdS, diverges due to contributions close to the boundary, so we regulate it with a cutoff  $R_b \gg 1$ . For short times, we find that the length behaves as  $L(t) \sim (t/\beta)^2$ , while for  $t/\beta \gg 1$ , then  $L(t) \sim t/\beta$ . The three key properties of the geodesic length in the AdS black hole case are:

1. Geodesics exist for arbitrarily long times.
2. The length of the geodesics always increases with time.<sup>2</sup>
3. After a short period of time of order  $\beta$ , the length increases linearly with time.

These three facts are some of the features that motivated the conjecture that the length of these geodesics is measuring the complexity holographically. Moreover, the linear growth is taken as an indication of the chaotic nature of the underlying microscopic theory [9, 10].

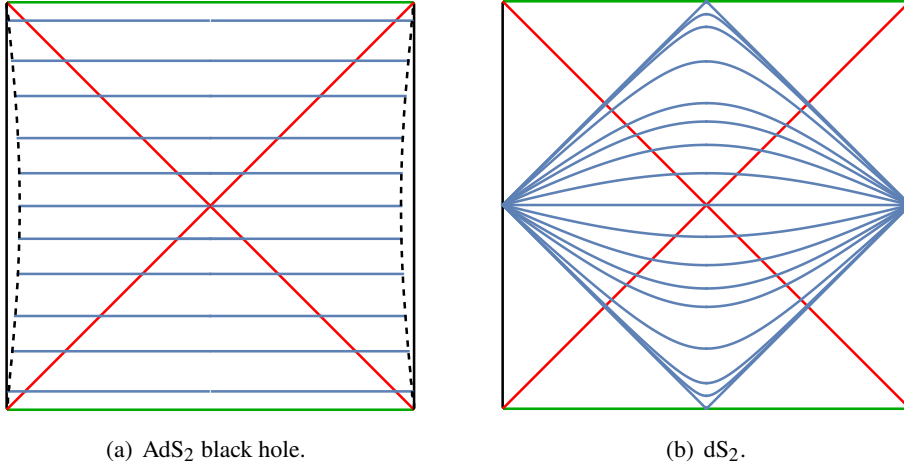


**Figure 2:** Penrose diagrams for the AdS<sub>2</sub> black hole and (half of) dS<sub>2</sub>. Geodesics are plotted in blue and  $R_b = 10$  is in dashed black in the AdS case. The red lines correspond to the horizons. Figure from [12].

This picture sharply contrasts with the geodesics in dS<sub>2</sub>. In this case, we have that  $f(r) = 1 - r^2$ . Evaluating the integrals (9) in this case, we obtain a completely different behaviour, shown in fig. 2(b), that can be summarised as follows,

$$L(t = 0)_{\text{dS}} = \pi. \quad (11)$$

As in the case of the AdS black hole, there is an infinite set of geodesics, parameterised by the continuous parameter  $P$ , but in this case,

1. All the geodesics are anchored at  $t = 0$ . There are no real, finite-length geodesics at  $t \neq 0$ .
2. The length of all the geodesics is the same and equal to half the length of the circle at  $t = 0$ , *i.e.*,  $L = \pi$ . It is interesting to note that the last geodesics are almost null everywhere but they touch the future/past infinities at a single point, giving a finite length of  $\pi$ .

<sup>2</sup>See [14] for saturation at time scales of order  $e^{S_0}$ , where  $S_0$  is the zero-temperature entropy.

3. Of course, there is no linear growth.

This result is somehow expected from the embedding space picture, where geodesics can be found as intersections of the dS hyperboloid with planes that pass through the origin. Nevertheless, it poses an interesting set of challenges. First, the two-point function in dS<sub>2</sub> at finite times is not zero, see eq. (5). So, according to the saddle-point approximation, we should be able to obtain it from a sum over geodesics, but there are no real geodesics. The oscillatory nature of the correlator would suggest that instead we should be considering complex geodesics. It would be interesting to find those and make a precise match with the two-point function. This would also open the interesting question of what is the role of these complex geodesics, if any, in holography. The second challenge is the interpretation of these geodesic lengths in terms of holography and complexity, but for that, we will embed dS inside AdS and compute the geodesics in the centaur geometry.

## 2.2 Geodesics in the centaur geometry

The spacetime in this case is given by

$$f(r)_{\text{centaur}} = \begin{cases} (1 - r^2), & -\infty < r < 0, \\ (1 + r^2), & 0 < r < \infty. \end{cases} \quad (12)$$

The geometry interpolates sharply between AdS for  $r > 0$  to dS for  $r < 0$ . At  $r = 0$ , the Ricci curvature jumps from  $R = +2$  to  $R = -2$ . There exist completely smooth interpolating spacetimes where the curvature changes smoothly in a region of size  $\varepsilon \ll 1$ , so this discontinuity in  $R$  is not problematic (see [3]). This geometry can be seen as a solution of a dilaton-gravity theory with dilaton potential  $U(\phi) = 2|\phi|$ . It can be shown that it also satisfies the null energy condition if viewed from a higher-dimensional perspective [15]. For other interesting features of the centaur geometry, see [3, 4].

For the purpose of this note, it is sufficient to remark that the geometry has an AdS boundary, so we can interpret the geodesics in this case in terms of holography.

The geodesics can be seen in fig. 3(a). As in the previous subsection, there exists a one-parameter family of geodesics. They exhibit some interesting features. As can be seen in fig. 3(b), a geodesic anchored at a positive time, goes through the past horizon, instead of the future horizon, as it is in the black hole case. This is a direct consequence of the fact of having dS in the interior and its holographic meaning remains to be understood.

The length of these geodesics as a function of the boundary time is given by

$$L(t)_{\text{centaur}} = \pi + 2 \operatorname{arcsinh} \left( \sqrt{(R_b^2 + 1) \cos^2 \left( \frac{\pi t}{\beta} \right) - 1} \right) = \pi + 2 \log \left( 2R_b \cos \frac{\pi t}{\beta} \right) + O(1/R_b^2), \quad (13)$$

where we restored the  $\beta$ -dependence. Note that the factor of  $\pi$  comes from the length of the part of the geodesics inside the dS patch. The last geodesic is, again, null everywhere and its length is given by  $\pi$ .<sup>3</sup>

Compared to the black hole case, this result is strikingly different — see fig. 4:

<sup>3</sup>This might be confusing by looking at eq. (13) close to  $t/\beta = 1/2$ , but this equation is only valid for  $R_b - \tan \pi|t|/\beta > 0$ . See [12].

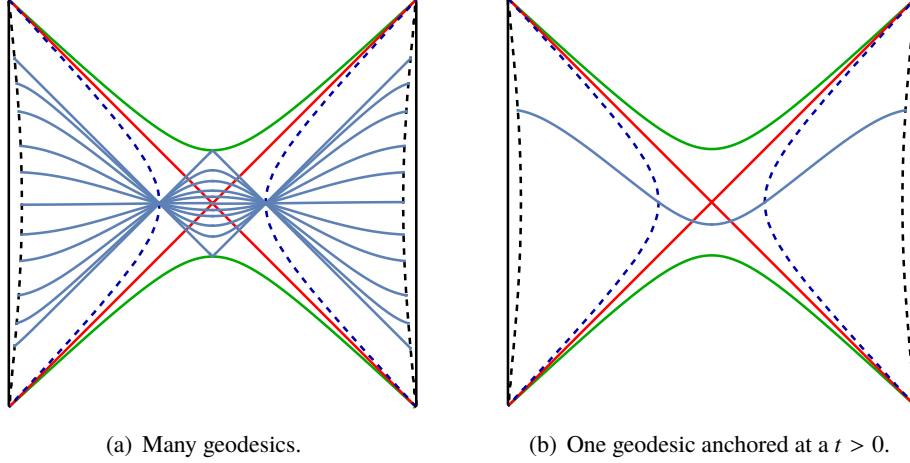


**Figure 3:** Penrose diagrams for the centaur geometry and geodesics anchored at different boundary times in blue, spanning the full range of times for which smooth spacelike geodesics of finite length exist. The dashed black line is the cutoff surface with  $R_b = 10$ . The dark blue dashed line is the interpolating line between the two geometries at  $r = 0$ . The red lines correspond to the horizons and the green ones correspond to  $r \rightarrow -\infty$ . Figure from [12].

1. There only exist real, finite-length geodesics for a short period of time of order  $\beta$ .
2. The length decreases with time.
3. There is no linear growth.

Both in terms of complexity or two-point correlator, the fact that the length decreases with time, points towards the idea that correlations in dS increase with time. This contrasts with the dissipative nature of black hole horizons where correlations decrease (exponentially) as time increases. After a time of order  $\beta$ , the geodesics reach the future/past infinity and then all real geodesics would have infinite length. As in the case of dS, there might be other complex geodesics in the centaur that would be interesting to find and characterise.

### 3. Outlook and discussion

As can be seen, the behaviour of geodesics in dS is both qualitatively and quantitatively different to those in AdS black holes.

For the black hole horizon, the linear growth in the geodesic length was associated to the maximally chaotic nature of the microscopic quantum theory [16]. In chaotic large  $N$  theories, there are two time-scales, that are parametrically large separated: the first one is dissipation time (given by  $\beta$  and associated to the exponential decay of two-point functions), and the second one is the scrambling time  $t_S \sim \beta \log N$ . Between these two scales, the behaviour of the four-points out-of-time-ordered correlator (OTOC), also supports the idea of maximal quantum chaos with [17]

$$\langle OTOC \rangle_\beta^{\text{BH}} = b_0 - \frac{b_1}{N} \exp\left(\frac{2\pi}{\beta} t\right) + \dots, \quad (14)$$

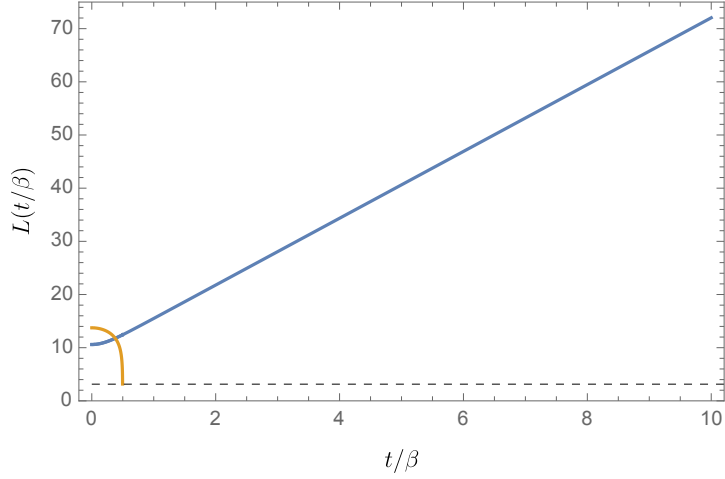


**Figure 4:** The length of geodesics as function of time for the AdS<sub>2</sub> black hole (in blue) and for the centaur geometry (in yellow).  $R_b = 100$ . Note that the length in the centaur case decreases with time up to times of  $t/\beta \sim 1/2$ , after which there are no more real geodesics with finite length. The last geodesic has length  $\pi$  that is shown in a dashed line. In contrast, the black hole length increases linearly with time for long times.

where  $b_{0,1}$  are positive, order-one constants. This correlator can also be computed in the centaur geometry [4] giving

$$\langle OTOC \rangle_\beta^{\text{centaur}} = c_0 - \frac{c_1}{N} \cos\left(\frac{2\pi}{\beta}t\right) + \dots, \quad (15)$$

where  $c_{0,1}$  are order-one constants. So, again the dS horizon does not seem to behave as chaotically as the black hole horizon. It is even hard to define a scrambling time in the centaur case, as the OTOC oscillates with time.

Both the geodesics and the OTOC point towards a different microscopic realisation of the cosmological horizon. In the case of the centaur, the holographic setup supports the idea of a microscopic RG flow in terms of SYK-like models [15]. Similar ideas were suggested in [18], where the dual theory to dS lives in the stretched horizon. The geodesic length in that case grows fast in a short period of time after it reaches future infinity. That rapid growth was said to be *hyperfast* – see also [19] – and it was suggested that an SYK model in a particular double-scaled limit might accomplish that kind of growth microscopically.

Finally, it would be interesting to consider the higher-dimensional case. Holographic complexities in  $dS_d$  computed from the stretched horizon were recently considered in [20]. In the case of the centaur, the flows from  $dS_d$  to  $AdS_d$  cannot be supported by matter obeying the null-energy condition [21]. However, it is possible to build flows from  $dS_d$  to  $AdS_2 \times S^{d-2}$  that do obey the null energy condition [22]. This is yet another indication that the microscopic realisation of the cosmological horizon might be of a more finite nature.

## Acknowledgements

We gratefully acknowledge discussions with Dionysios Anninos, Diego Hofman, Sameer Sheorey and David Vegh. This note is based on work in collaboration with Shira Chapman and Erik



David Kramer. We would like to also thank the organisers of the Workshop on Quantum Features in a de Sitter Universe for the opportunity to present these results. This work is funded by the Royal Society under the grant “The Resonances of a de Sitter Universe” and the ERC Consolidator Grant N. 681908, “Quantum black holes: A microscopic window into the microstructure of gravity”.

## References

- [1] M. Spradlin, A. Strominger and A. Volovich, *Les Houches lectures on de Sitter space*, in *Les Houches Summer School: Session 76: Euro Summer School on Unity of Fundamental Physics: Gravity, Gauge Theory and Strings*, pp. 423–453, 10, 2001, [hep-th/0110007](#).
- [2] D. Anninos, *De Sitter Musings*, *Int. J. Mod. Phys. A* **27** (2012) 1230013 [[1205.3855](#)].
- [3] D. Anninos and D. M. Hofman, *Infrared Realization of  $dS_2$  in  $AdS_2$* , *Class. Quant. Grav.* **35** (2018) 085003 [[1703.04622](#)].
- [4] D. Anninos, D. A. Galante and D. M. Hofman, *De Sitter Horizons & Holographic Liquids*, *JHEP* **07** (2019) 038 [[1811.08153](#)].
- [5] J. Louko, D. Marolf and S. F. Ross, *On geodesic propagators and black hole holography*, *Phys. Rev. D* **62** (2000) 044041 [[hep-th/0002111](#)].
- [6] V. Balasubramanian and S. F. Ross, *Holographic particle detection*, *Phys. Rev. D* **61** (2000) 044007 [[hep-th/9906226](#)].
- [7] M. Cvitković, A.-S. Smith and J. Pande, *Asymptotic expansions of the hypergeometric function with two large parameters—application to the partition function of a lattice gas in a field of traps*, *Journal of Physics A: Mathematical and Theoretical* **50** (2017) 265206.
- [8] S. Ryu and T. Takayanagi, *Holographic derivation of entanglement entropy from AdS/CFT*, *Phys. Rev. Lett.* **96** (2006) 181602 [[hep-th/0603001](#)].
- [9] L. Susskind, *Computational Complexity and Black Hole Horizons*, *Fortsch. Phys.* **64** (2016) 24 [[1403.5695](#)].
- [10] D. Stanford and L. Susskind, *Complexity and Shock Wave Geometries*, *Phys. Rev. D* **90** (2014) 126007 [[1406.2678](#)].
- [11] S. Chapman and G. Policastro, *Quantum computational complexity from quantum information to black holes and back*, *Eur. Phys. J. C* **82** (2022) 128 [[2110.14672](#)].
- [12] S. Chapman, D. A. Galante and E. D. Kramer, *Holographic complexity and de Sitter space*, *JHEP* **02** (2022) 198 [[2110.05522](#)].
- [13] A. R. Brown, H. Gharibyan, H. W. Lin, L. Susskind, L. Thorlacius and Y. Zhao, *Complexity of Jackiw-Teitelboim gravity*, *Phys. Rev. D* **99** (2019) 046016 [[1810.08741](#)].
- [14] L. V. Iliesiu, M. Mezei and G. Sárosi, *The volume of the black hole interior at late times*, [2107.06286](#).

- [15] D. Anninos and D. A. Galante, *Constructing  $AdS_2$  flow geometries*, *JHEP* **02** (2021) 045 [2011.01944].
- [16] J. Maldacena, S. H. Shenker and D. Stanford, *A bound on chaos*, *JHEP* **08** (2016) 106 [1503.01409].
- [17] S. H. Shenker and D. Stanford, *Black holes and the butterfly effect*, *JHEP* **03** (2014) 067 [1306.0622].
- [18] L. Susskind, *Entanglement and Chaos in De Sitter Holography: An SYK Example*, *Journal of Holography Applications in Physics* **1** (2021) 1 [2109.14104].
- [19] E. Shaghoulian, *The central dogma and cosmological horizons*, *JHEP* **01** (2022) 132 [2110.13210].
- [20] E. Jørstad, R. C. Myers and S.-M. Ruan, *Holographic Complexity in  $dS_{d+1}$* , 2202.10684.
- [21] B. Freivogel, V. E. Hubeny, A. Maloney, R. C. Myers, M. Rangamani and S. Shenker, *Inflation in  $AdS/CFT$* , *JHEP* **03** (2006) 007 [hep-th/0510046].
- [22] D. Anninos, D. A. Galante and B. Mühlmann, *to appear*, .